Paper Number 2018-01-1452

Comparison of 1-D Modelling Approaches for Wankel Engine Performance Simulation and Initial Study of the Direct Injection Limitations

Author, co-author (Do NOT enter this information. It will be pulled from participant tab in MyTechZone)

Affiliation (Do NOT enter this information. It will be pulled from participant tab in MyTechZone)

Abstract

Recent interest in the possible use of Wankel engines as range extenders for electric vehicles has prompted renewed investigations into the concept. While not presently used in the automotive industry, the type is well established in the unmanned aerial vehicles industry, and several innovative approaches to sealing and cooling have recently been developed which may result in improved performance for ground vehicle applications.

One such UAV engine is the 225CS, a 225 cc/chamber single-rotor engine manufactured by Advanced Innovative Engineering (UK) Ltd. To be able to analyse the parameters, opportunities and limitations of this type of engine a model was created in the new dedicated Wankel modelling environment of AVL BOOST. For comparison a second model was created using the established method of modelling Wankel engines by specifying an 'equivalent' 3-cylinder 4-stroke reciprocating engine. The output from both of these models was evaluated using engine test data supplied by Advanced Innovative Engineering (UK) Ltd. The model created in the dedicated Wankel environment was found to fit the experimental data more closely.

The model was then used to evaluate the impact on performance and fuel economy of applying direct injection to a Wankel rotary engine. This potential is because the nozzle can be situated in the cold side of the trochoid housing, taking advantage of the longer intake phase of the Wankel in turn permitting lower delivery pressures (the intake 'stroke' having 270 degrees of eccentric shaft rotation vs. 180 degrees for the reciprocating engine), plus the fact that the injector can be shielded from combustion pressure and hot burned gases. As it was found to be more accurate, the dedicated Wankel model was used to analyse the interrelationships between injector position, injection pressure and engine speed.

Although a number of assumptions were required, and these will affect the accuracy of the model, the results provide a reasonable preliminary assessment of the feasibility of applying direct injection to the 225CS engine. A notable finding was that injection pressures of approximately 4.5 bar should be sufficient to supply fuel at all engine speeds and that the optimum position for the injector (for maximum fuel injection) corresponded to a position defined by the rotor apex tip at 597 degrees of eccentric shaft rotation after top dead centre firing. The advantage of both the injection pressure and injector location suggests a less complex fuel system design (compared to equivalent reciprocating systems) is possible at a reduced cost.

Introduction

The Wankel engine

In 1929 Felix Wankel was awarded the first patent for his rotary engine design [1]. Unlike conventional engines that rely on reciprocating pistons to drive a crank shaft, the Wankel engine creates rotational motion directly through an eccentric rotary design where the moving parts always rotate in the same direction. The Second World War stalled the development and it was not until 1957 that a motorcycle manufacturer, NSU took notice of Wankel's design and together they created the first operational prototype [2]. The engine performed as expected with high specific power, low vibration and was capable of engine speeds in excess of 25,000 rpm without failure [3]. However, there were flaws and much more work was required before the engine could be seen as a viable power plant for automotive applications. Despite this NSU licensed the design to many prominent automotive manufacturers such as Daimler-Benz, General Motors, Citroen, Rolls Royce and Toyo Kogyo (now Mazda), all of whom invested heavily in the concept [3]. Only Mazda produced the engine in significant numbers and as emission regulations around the world tightened from the 1970's they limited the use of Wankel engines to their performance models, finally ceasing production of the RX-8 in 2012, the last mass produced car featuring a Wankel engine. Today, Wankel engines find use only in bespoke applications such as UAVs (unmanned aerial vehicles), and auxiliary power units [4] [5].

Operation

The Wankel engine operates with the same Otto cycle as a conventional four-stroke reciprocating engine but their kinematic mechanisms are fundamentally different, shown in Figure 1. The modern form of the Wankel engine consists of a moving three pointed rotor (similar in shape to a Reuleaux triangle) set within a stationary epitrochoidal housing which is flanked by two side housings. An internal gear on the rotor meshes with a stationary gear on the side housing and provides the phasing of the engine. An eccentric shaft with an offset equal to the distance between the centres of the phasing gears runs through the centre of the rotor. This setup facilitates an eccentric orbit that ensures the apex seals are in constant contact with the epitrochoidal housing, creating three sealed chambers. The gearing rotates the eccentric shaft three times for every single rotation of the rotor, making a complete cycle 1080° of eccentric shaft rotation [6]. Since the shape of the rotor allows three cycles to take place simultaneously the engine experiences one combustion event for every rotation of the eccentric shaft which provides a very high volumetric efficiency and consequently

considerable power output relative to the size of the engine [3]. As the rotor turns, ports in the epitrochoidal or side-housing are sequentially exposed and covered providing the equivalent to 'valve timing' in a conventional 4-stroke engine and removing the need for an exogenous valve train. This unique design delivers an engine with far fewer moving parts than a reciprocating engine, resulting in smaller inertial forces and lower mechanical stresses. Wankel engines give a characteristically smooth performance and have the ability to operate at very high engine speeds [7].

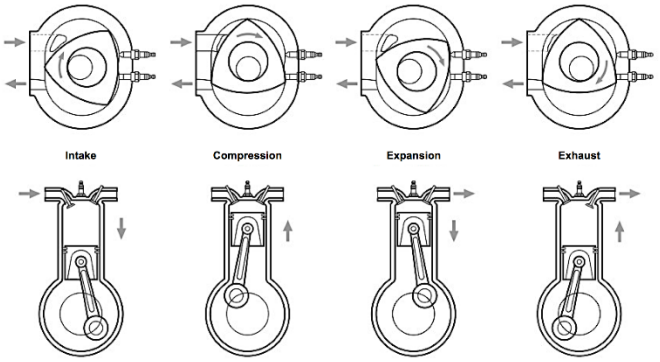

Figure 1: Four-stroke cycle of the Wankel rotary engine (above) and reciprocating engine (below). The correspondence of the intake, compression, expansion and exhaust phases between both designs are illustrated. [Adapted from [8]]

Future Potential

Increasingly stringent emissions regulations have resulted in growing research efforts to develop hybrid and fully electric vehicles. The USA became the first country to introduce emissions regulations on a national level with the Clean Air Act of 1963 resulting in reductions in engine pollutants over the coming decades [9]. Since then, government bodies and international organizations such as the European Union (EU) have further increased regulation and assessment of vehicle emissions. In 2017 both France and the UK pledged to ban all sales of new petrol and diesel cars by the year 2040, following earlier announcements of intent made by the Netherlands and Denmark [10]. The Euro 7 emissions (likely to be implemented in 2021) will legislate fleet average emissions of only 95 grams of CO_2 per kilometre [11], a figure not achieved by most currently available hatchbacks [12]. The replacement of internal combustion powertrains in their conventional form is therefore imminent.

As early as 1995 the Wankel engine was recognised as a potential range extender for series hybrid electric vehicles (or range-extended electric vehicles), due to its compact design and low Noise, Vibration and Harshness (NVH) characteristics [13]. In 2008 FEV produced a series hybrid electric powertrain utilising a Wankel range extender. The engine of the baseline vehicle (a Fiat 500) was replaced with an electric motor, a lithium-ion battery pack and a small single rotor 47hp Wankel engine produced by the German rotary engine manufacturer Aixro [14]. The Wankel engine increased the range from 100 km to 300 km. Another similar project in 2010 saw a collaboration between Audi and AVL convert an Audi A1 into a plug-in hybrid with a Wankel range extender placed under the floor level of the boot. It has been estimated that the use of a Wankel range extender in a passenger vehicle would incur an additional cost of ~£2500 per vehicle, given a unit production greater than 100,000 [15]. Despite the growing commercial interest in their application as range extenders in hybrid vehicles, to date no model has reached the market.

Direct Injection

After the successful application of direct injection (DI), first for reciprocating compression ignition (CI) engines and then in reciprocating spark ignition (SI) engines, it is anticipated that DI may have potential to further advance the design of Wankel engines. In DI engines, the fuel is injected directly into the working chamber where vaporising the fuel reduces the charge temperature resulting in the potential to apply higher compression ratios, accordingly increasing the power output and improving fuel economy of the engine.

There are two modes of DI: homogeneous charge, where the fuel is injected during the intake stroke to ensure the fuel and air are well mixed at the time of combustion, and stratified charge, where fuel is injected later to create an overall lean charge with a rich core. Although the stratified charge mode generally offers superior fuel economy the additional oxygen present in the exhaust stream, as a result of the overall lean mixture, prevents the use of a three-way catalytic converter to remove the oxides of nitrogen (NOx) [16]. Therefore, the clear majority of DI systems used in gasoline engines operate in exclusively the homogeneous mode when warmed up [17].

It is worth noting that applying DI to a Wankel engine is not a completely new concept and numerous prototypes were created by several companies from the 1970s to the 1990s. Curtiss-Wright experimented with various direct injection layouts for aero engines [3], Daimler-Benz developed a four rotor Wankel engine with mechanical DI for use in the famous Mercedes-Benz C111 experimental car [18] and John Deere created a family of DI engines known by the acronym SCORE (Stratified Charge Omnivorous Rotary Engine)[19]. However, all these engines employed high pressure stratified charge injection and not the homogeneous charge injection being investigated in this paper.

Focus of this Work

Peden's work [20], on which this paper is based, attempted to first establish whether the Wankel domain available in AVL BOOST software was a reliable platform for modelling Wankel engines by comparing with the earlier modelling approach of adjusting reciprocating engine software. The model followed the specification of the Advanced Innovative Manufacturing (AIE) Ltd. designed 225CS Wankel engine (Figure 2). This has been used in drones, for various light-industrial purposes and there is now an interest in its use as a range extender for hybrid-electric vehicles. AIE's primary focus revolved around the potential of applying low pressure homogeneous charge DI to the 225CS to improve overall performance (notably fuel consumption and emissions). After the Wankel domain model was verified with experimental data, the pressure trace for the working chamber was then used to study the interrelationships of injection pressure, injector position and engine speed when applying DI to the engine. This provided an insight into the potential benefits and limitations of applying this technology to improve the power output and fuel economy of the Wankel engine.

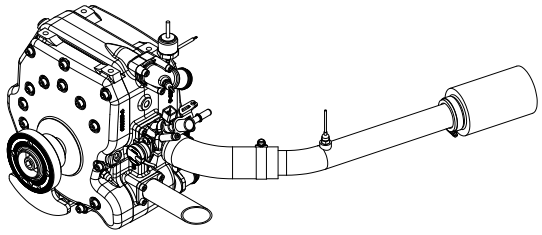

Figure 2: Computer Aided Design (CAD) Image of the AIE (UK) Ltd. 225CS Wankel engine with intake and exhaust pipe fitted (inlet and injector above, exhaust below)

Methodology

Engine Geometry

Wankel Model Geometry

The geometry of the Wankel engine can be characterised by three fundamental dimensions: the generating radius (R), eccentricity (e) and housing depth (b). The generating radius and eccentricity are illustrated in Figure 3, while the housing depth corresponds to the in-page dimension.

In order to prevent pressure loss during combustion each working chamber needs to be isolated from the next so the equations used here to characterise the geometry include an offset (or parallel transfer) to account for the sprung seals at the apexes of the rotor. The offset for the housing (a) is equal to the radius of the apex seal (highlighted in Figure 4). In addition, a rotor clearance parameter (a'),

$$a' = a - S_p \tag{1}$$

S_p (being the minimum clearance between the rotor and housing) is also specified.

Modelling the 225CS engine in BOOST requires relationships for the instantaneous volume (for combustion) and instantaneous surface area (for heat transfer).

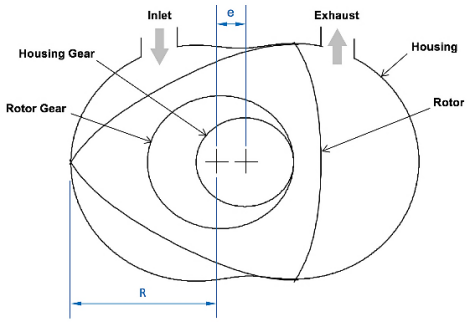

Figure 3: Schematic of Wankel engine cross-section, highlighting the generating radius (R) and eccentricity (e) dimensions. Direction of rotation for this engine is counterclockwise

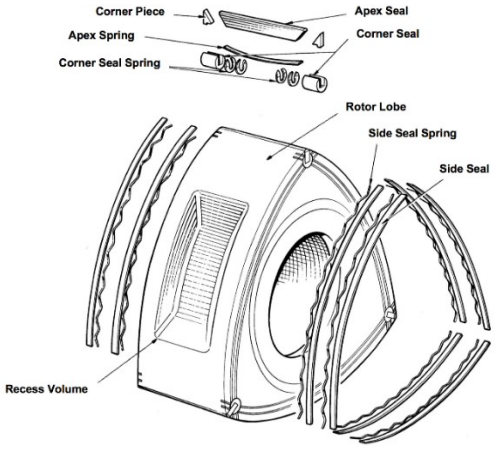

Figure 4: Exploded view of a generic Wankel Rotor. [Adapted from [22]]

The instantaneous volume (V') with respect to the shaft angle (α) was calculated using the following, adapted from [6]:

$$V' = V'_{min} + \frac{\sqrt{3}}{2} e(R_1 + R_2) b \left\{1 - \sin\left(\frac{2}{3}\alpha + \frac{\pi}{6}\right)\right\} \tag{2}$$

Where, $R_1 = R + a$, $R_2 = R + a'$ and V'_{min} (minimum volume) was calculated using:

$$V'_{min} = \left\{\frac{\pi}{3}e^2 + \frac{{R_1}^2 - {R_2}^2}{3}\pi \ldots + 2eR_2 \cos\varphi_{max} + \left(\frac{2}{9}{R_2}^2 + 4e^2\right)\varphi_{max} \ldots - \frac{\sqrt{3}}{2}e(2R_1 + R_2)\right\} b + V_{recess} \tag{3}$$

Where V_{recess} is the volume of the recess on the rotor lobe (shown in Figure 4) and φ_{max} is the angle between the normal of the rotor apex and the normal of the housing, known as the maximum angle of oscillation and given by:

$$\varphi_{max} = \sin^{-1}\left(\frac{3e}{R}\right) \tag{4}$$

The instantaneous surface area of a Wankel combustion chamber (A) can be determined as the sum of the rotor lobe area (A_L), side housing area (A_S) and epitrochoidal housing area (A_E), the latter two dependent on the eccentric angle:

$$\frac{dA}{d\alpha} = A_L + \frac{dA_S}{d\alpha} + \frac{dA_E}{d\alpha} \tag{5}$$

The rotor lobe area is constant throughout the combustion cycle and can be approximated by multiplying the length of the curved profile of a single lobe by the housing depth [22]:

$$A_L = R_x(2\beta)b \tag{6}$$

Equations used to find the equivalent radius (R_x) and half angle (β) can be found in Appendix I. In reality, the profile of the 225CS rotor lobe is altered to prevent contact with the minor axis of the epitrochoidal housing, however this is expected to have little influence on the overall surface area as it is likely to be moderated by the additional surface area of the recess volume.

The instantaneous side area of the rotor housing (F) was calculated using the following, adapted from [6]:

$$\mathrm{F} = \frac{dA_s}{d\alpha} = \frac{\pi}{3}e^2 + eR\left\{2\cos\varphi_{max} - \frac{3\sqrt{3}}{2}\sin\left(\frac{2}{3}\alpha + \frac{\pi}{2}\right)\right\} + \left(\frac{2}{9}R^2 + 4e^2\right)\varphi_{max} \tag{7}$$

Calculating the instantaneous epitrochoidal area is more complex and requires a numerical approach such as the parametric rectification method used by Tomlinson [23]. Here, for simplification, a recognised approximation method that simplifies the Wankel engine combustion chamber as a cube of length equal to the rotor profile, width equal to the housing depth and height that varies sinusoidally with the chamber volume was used. The following equation was altered from [22]:

$$\frac{dA_E}{dV'} = 2\left(\frac{\left(\frac{dV'}{d\alpha}\right)}{b} + \frac{\left(\frac{dV'}{d\alpha}\right)}{R_x(2\beta)} + R_x(2\beta)b\right) \tag{8}$$

Equivalent Reciprocating Geometry

A geometrically equivalent reciprocating engine needs to have the same instantaneous volume and surface area as the Wankel engine it is intended to replicate. This was achieved by solving a cubic for the minimum volume and area, the derivation of which can be found in Appendix I. This method allowed the piston bore, crank radius and combustion chamber height to be specified to return the best possible match to a given Wankel engine.

Using this approach allowed the maximum and minimum volume to correspond absolutely with the Wankel geometry. To ensure near-sinusoidal volume change, which is characteristic of a Wankel engine, the connecting rod was set at 2 m (creating a large connecting rod to crank radius). Figure 5 shows the correspondence between the volumes of the reciprocating and rotary model.

However, due to fundamental mechanistic differences it is impossible to achieve an equally good match for surface area. The method used here does however ensure that the surface area is equal at top dead centre (TDC) for both models (0° and 540° of eccentric shaft rotation for a Wankel engine and 0° and 360° of crank shaft rotation for a reciprocating engine), is shown in Figure 6.

Figure 7 shows a comparison of the surface to volume ratio between the reciprocating and Wankel models.

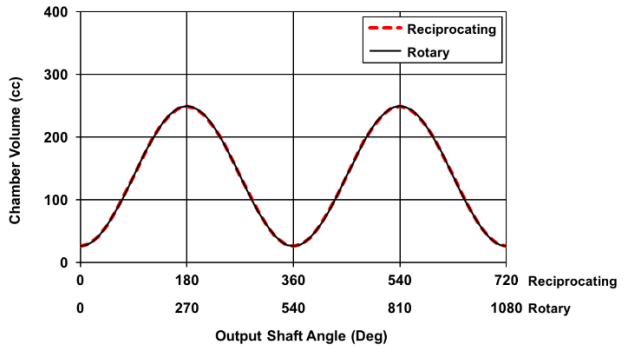

Figure 5: Working chamber volume vs. angle of shaft rotation for the Wankel and reciprocating models

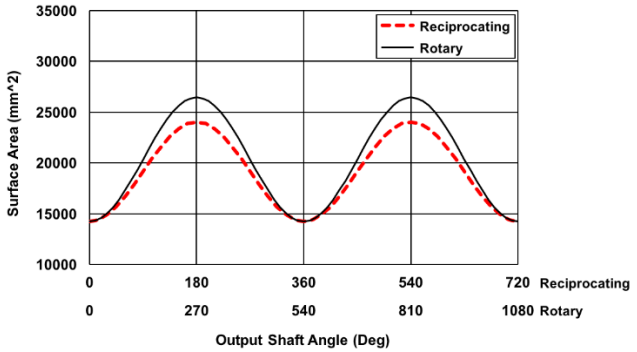

Figure 6: Working Chamber surface area vs. angle of shaft rotation for the Wankel and reciprocating models

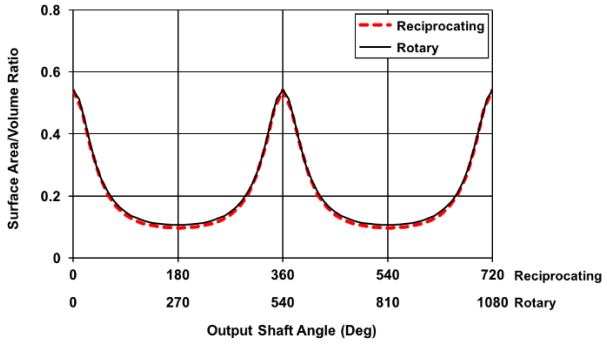

Figure 7: Working chamber surface/volume ratio vs. angle of shaft rotation for the Wankel and reciprocating models

Modelling the engine in the rotary engine modelling environment

AVL BOOST was used to model the engine as it is currently the only available gas dynamics software to feature a dedicated rotary engine modelling environment. BOOST is a one-dimensional multilevel programme designed to simulate variable engine operating conditions with real-time processing. The 225CS was modelled in BOOST using standard elements available in the software, as illustrated in Figure 8.

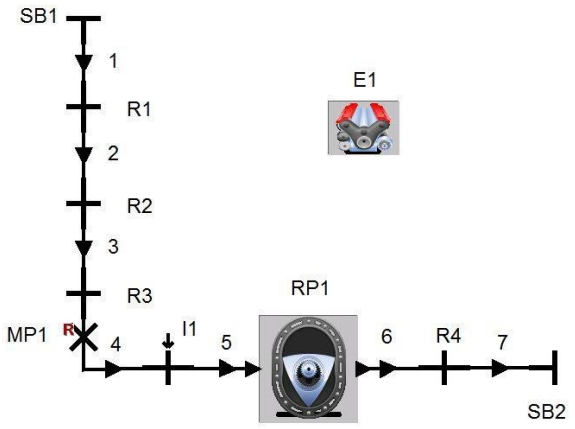

Figure 8: AVL BOOST model developed in the rotary domain of the software for the AIE (UK) Ltd. 225CS

Port Specifications

As mentioned in the introduction the Wankel design relies on the apices of the rotor to govern gas exchange. Therefore, instead of specifying valve lift curves the flow is characterised by a fixed discharge coefficient for intake and exhaust over an output shaft range of 360° (the eccentric interval between rotor apexes) as shown in Figure 9. The intake and exhaust port locations were measured directly from the engine.

Unlike a reciprocating engine where the intake and exhaust ports are circular to facilitate a valve, the ports in the 225CS are oblong in shape (geometrically referred to as a 'stadium'). Therefore, to achieve the same cross-sectional area a circular port with the equivalent area was specified in the model.

The discharge coefficients for intake and exhaust have a significant influence on the gas exchange calculations. Ideally, the coefficients would be derived experimentally by recording measurements while air is forced through each orifice, however these experiments have not been conducted on the 225CS. Tartakovsky *et al*. [4] adopted a computational approach for approximating the discharge coefficients of two Wankel aero engines with displacements of 294 cc and 350 cc. Virtual blowing simulations were conducted using ANSYS Fluent CFD software. At wide open throttle (WOT) discharge coefficients of 0.92 and 0.95 were recorded for the intake and exhaust, respectively. Since the engines were similar in displacement to the 225CS, the discharge coefficients from Tartakovsky's analysis were used in the models here.

For the 225CS, the intake and exhaust ports are open simultaneously between 469° and 597° of the eccentric shaft rotation, as illustrated in Figure 9. The scavenging process for Wankel engines is not well documented making accurate predictions difficult [7]. In this model, the standard 'perfect mixing' scavenging model was implemented which assumed gas flowing into the chamber was instantly mixed with the chamber contents and that the gas leaving the chamber had the same composition as the charge in the chamber. The validity of this simplification is unclear and producing a more realistic model of the scavenging process will be an area of focus for future work.

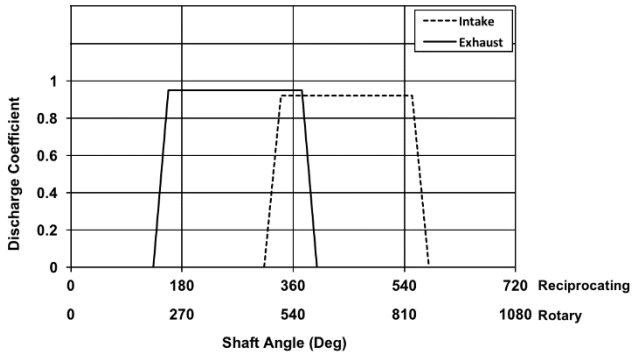

Figure 9: Engine timing and discharge coefficients for intake and exhaust as a function of shaft rotation

Combustion

The combustion characteristics were modelled using a heat release approach, where the total heat release during combustion was subject to the mass fraction of fuel burned in the combustion chamber and the lower heating value of the fuel (~43500 kJ/kg for gasoline). The Wiebe function was used to predict this [24]:

$$x_b = 1 - exp\left\{-a\left(\frac{\theta - \theta_0}{\Delta\theta}\right)^{m+1}\right\} \quad (9)$$

Where x_b is the cumulative mass fraction, θ is the shaft angle, θ_0 is the start of combustion and $\Delta\theta$ is the combustion duration. The constants a and m are adjustment parameters that determine the character of the rate of heat release (ROHR) and mass fraction burned curves. Specifically, parameter a characterises the completeness of combustion (with a value of 6.9 required for complete combustion) and the Wiebe exponent m influences the shape of the response [25].

For accurate engine simulations, values for the adjustment parameters may be derived from measured combustion chamber pressure over an engines speed and load range. In the absence of such data, here an approximate constant for each was selected based on available published data for Wankel engines (a = 5 and m = 2) [26] [27].

The flame propagation speed and shape of the combustion chamber largely determine the heat release characteristics of gasoline engines. The high turbulence levels of Wankel engines result in relatively high flame propagation speeds [3]. The unfavourable shape of the combustion chamber (especially at TDC) is detrimental to

combustion due to flame quenching at the narrow leading and trailing edge of the combustion chamber. The 1D software used here cannot account for this and therefore using such a model to predict combustion in a Wankel engine has its limitations.

Heat Transfer

Heat transfer is responsible for the most significant loss of energy in an internal combustion engine [27]. Modelling heat transfer is particularly challenging as there are many paths and modes in which heat can transfer. A recognised approach to this challenge is to use the Woschni correlation with temperature data for the different elements of the combustion chamber over the speed and load range of an engine [29]. However, the data required for the 225CS was not available and therefore an approximation was used instead.

Results from a temperature indicating paint (TIP) test revealed a maximum temperature of ~300° on the rotor lobe face at 7500 rpm. As this was the only temperature data available for the 225CS it was assumed all internal surfaces were at this temperature over the speed and load range of the engine, since any other predictions would have been speculative until further tests are completed. Assuming uniform temperature throughout the working chamber is evidently unrealistic [30], this assumption therefore considerably limits the fidelity of the model as heat transfer plays a crucial role in the performance of Wankel engines.

A sensitivity analysis was conducted to investigate the influence of heat transfer and the result is shown for torque in Figure 10. Changing the temperature of the internal surface of the combustion chamber from 300°C to 150°C increased the power and torque output by ~2.8 bhp and ~3.3Nm respectively, while disregarding the heat transfer altogether increased both power and torque considerably more. Therefore, although the current approach is sufficient as an approximation, more temperature data is required to develop a more accurate model.

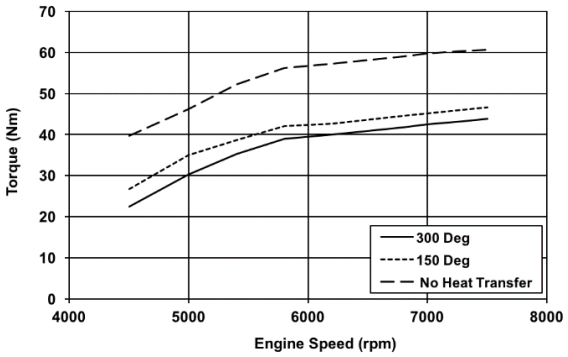

Figure 10: Predicted torque vs. engine speed for the rotary model. The relationships shown display the sensitivity of the heat transfer model from no heat transfer to working chamber surface temperatures of 300 °C

Leakage and Blow-By

In AVL BOOST combustion chamber leakage is separated into two core components. Blow-by, the movement of gas from the combustion chamber to the inner core (via the side seals) and apex seal leakage, the movement of gas from chamber to chamber across the apex seals. In the initial model set-up only blow-by leakage was considered.

The extent of blow-by is dependent on an effective blow-by gap and the mean crankcase pressure (core pressure for a Wankel engine). The degree of leakage can be measured directly from the engine using a leakdown test, which involves pressurising the combustion chamber and recording the total leakage as a percentage [31]. Unfortunately, this test has not been conducted on the 225CS and therefore a method of approximating the extent of blow-by was required.

Unlike conventional Wankel engines that are either closed-loop, oil-cooled or forced-air-cooled the 225CS utilises AIE's patented Self-Pressurised Air Rotor Cooling System (SPARCS) to cool the rotor [32]. The system exploits the pressurised blow-by gases which migrate to the engine core through the side seals. The dense pressurised gas is continually recirculated between the rotor and a heat exchanger via an internal fan to reject heat from the engine. The novel design provides an effective way of removing heat from the engine while reducing oil consumption, however it poses an additional challenge for modelling the blow-by of the engine.

As with the crankcase of a conventional reciprocating engine, typically the core of a Wankel engine is vented into the intake manifold via a one-way valve. This process regulates the pressure in the core to a fixed value depending on the specification of the valve and can be input as a constant in the BOOST program. Due to the peculiarity of the SPARCS system the core pressure is not vented and instead the pressure is allowed to build as engine speed increases, as shown by the experimental pressure data in Figure 11. A polynomial trend was fitted to the data (indicated as the solid line 'Core Pressure') so that an approximation of the pressure over the engine speed range was available. As BOOST cannot specify the core pressure with respect to engine speed the value had to be manually altered for each iteration of the model.

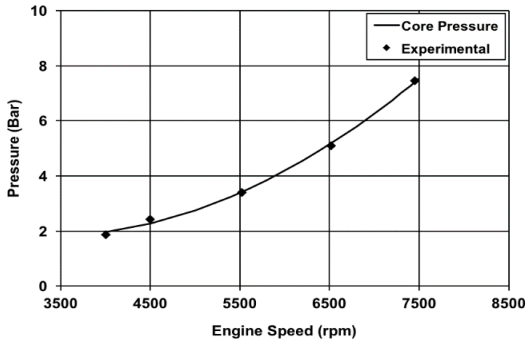

Figure 11: Core pressure of 225CS vs. engine speed. The polynomial relationship for core pressure and the experimental values it is based on are plotted

Data regarding the dimensions of the blow-by gap between combustion chamber and the rotor core for Wankel engines is unavailable in literature, therefore, a relationship used to determine the typical fitting clearance of a reciprocating engine made from similar materials as the 225CS was used [33]. Using this approximation, an effective blow-by gap of approximately 0.01 mm was calculated and used in the model. This simplification is likely to be a source of considerable error due to the complex sealing characteristics of a Wankel engine compared with a reciprocating

engine and future work should consider a more accurate method for determining the effective blow-by gap.

Moreover, the combustion chamber volumes influencing the compression ratio do not account for openings in the housing (such as spark plugs and potential injectors), this should therefore be accounted for in future models once more engine data is acquired.

Friction

Frictional loss, defined as the difference between the indicated work and the brake work, is an important factor when modelling the performance of an engine. For a Wankel engine frictional loss can be attributed to losses due to eccentric shaft friction, rotor friction (due to seals rubbing on the housing) and losses due to auxiliary components.

In BOOST the friction is determined by applying a friction mean effective pressure (FMEP) to the model. Ideally, data for the FMEP would be obtained from motoring tests of the engine, which would involve rotating the output shaft of the engine via an electric motor without combustion taking place. To account for the thermal expansion characteristics of the engine the procedure should take place with the engine heated to operational temperature [34]. These tests have not yet been completed for the 225CS and a method for approximating the FMEP had to be employed instead.

Friction equations and characteristics for Wankel engines are not well documented in the literature, with most methods of frictional analysis based on empirical data [35]. Conversely, the frictional characteristics of reciprocating engines are well known. However, these characteristics cannot be applied directly to a Wankel engine since the relationships account for friction in a valve train (which is not present in a Wankel engine). Therefore a 4-stroke relationship would likely overestimate the friction of the 225CS. Instead, a relationship derived for a piston ported 2-stroke engine was used. Like a Wankel engine a piston ported 2-stroke engine has fewer moving parts than a 4-stroke since the gas exchange is governed by the piston, thus avoiding the requirement of valves.

The following empirical relationship has been proven to correlate well with experimental observations on various small two-stroke engines and was used to approximate the FMEP (Pa) of the 225CS [36]:

$$FMEP = 150 L_{st} N \tag{10}$$

Where L_{st} is the engine stroke length in meters and N is the engine speed in revolutions per minute. The relationship also assumes an output shaft with rolling element bearings, as is the case with the 225CS.

A plot of the linear friction relationship is shown in Figure 12. Using this relationship resulted in mechanical efficiencies of ~96.7% at low engine speeds and ~97% at high engine speeds. Mechanical efficiency was calculated with the following [24]:

$$\eta_m = \frac{BMEP}{IMEP} \tag{11}$$

Where $BMEP$ is the Brake Mean Effective Pressure and $IMEP$ is the Indicated Mean Effective Pressure.

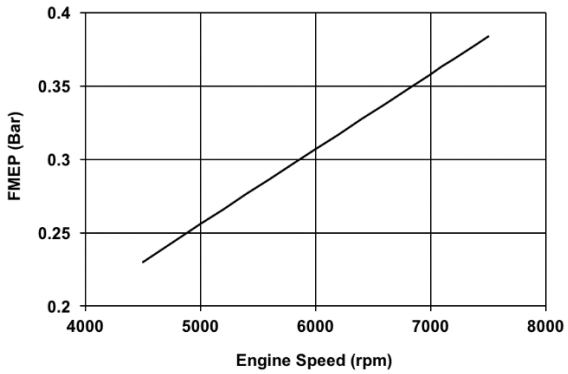

Figure 12: Approximation of FMEP vs. engine speed for the AIE 225CS

Equivalent Reciprocating Model

Straightforward use of the reciprocating domain in AVL BOOST to model a Wankel engine is impossible. To model all three working chambers of the Wankel engine required three cylinder elements, as illustrated in Figure 13. The shape of the combustion chamber is irrelevant since the model is one dimensional. Modelling cylinder elements in AVL BOOST requires individual connections to the inlet and exhaust of the cylinder elements. However, in a Wankel engine the working chambers share common intake and exhaust channels. To mitigate the effect of splitting the main inlet channel, flow connections 5-13 shown in Figure 13 for the reciprocating model were specified as the minimum allowable length in the BOOST software of 3 mm. In addition, it was necessary to use plenum elements at the junctions to ensure continuous flow and equal air distribution through the main inlet channel and outlet duct, as Wendeker [21] has previously used.

Since a reciprocating engine 4-stroke Otto cycle takes place over 720° (two-thirds that of a Wankel engine Otto cycle), data entered into the model was scaled accordingly. Furthermore, the simulation was run at two-thirds the actual engine speed so that there were the same number of combustion events for a given time period. To account for this, outputs from the model dependent on engine speed such as power were corrected from the brake mean effective pressure (BMEP) at the end of each simulation.

The equivalent reciprocating model used similar combustion, heat transfer, leakage and friction relationships as previously mentioned. However, it is worth noting that the large velocity changes induced by the rotor of a Wankel engine may render the heat transfer correlations for the reciprocating model unrepresentative of the Wankel engine [30].

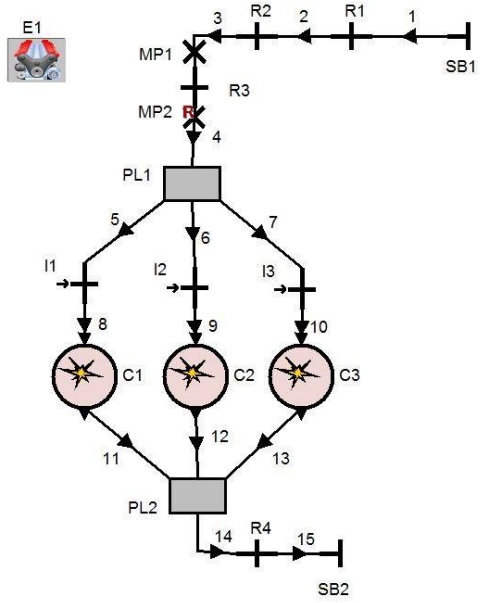

Figure 13: AVL BOOST model developed in the reciprocating domain of the software for the AIE 225CS

Injection Parameters

In order to facilitate investigation of direct injection parameters, once the BOOST model had been validated pressure traces of the combustion chamber were exported for an engine speed of 5000 rpm and 7500 rpm (an example can be found in Appendix III). The pressure trace was then used to determine the instantaneous differential pressure between the injector and the working chamber with respect to the eccentric shaft angle. The instantaneous flow rate of the injector ($\frac{dV}{dt}$) for a given position on the epitrochoidal housing was then calculated using the following relationship [37]:

$$\frac{dV}{dt} = D_d A \sqrt{\frac{2}{\rho}\left(P_{inject} - P_{chamber}\right)} \tag{12}$$

Where D_d is the discharge coefficient of the injector, A is the cross-sectional area of the nozzle, ρ is the density of the fuel and $P_{inject} - P_{chamber}$ is the differential pressure between the injector and working chamber.

The current port fuel injection (PFI) system of the 225CS employs a standard Bosch EV-14 automotive fuel injector regulated to 3 bar. For the purpose of this project it was assumed that the EV-14 injector (with its current specification [39]) would be applied to the housing for direct injection. From OEM data, it was possible to determine the flow area of the injector over the speed range of the engine. A polynomial relationship was derived to represent the data in the simulation, as in Figure 14.

Since no discharge coefficient was known for the injector an approximation of 0.66 was assumed based on typical gasoline low pressure injection discharge coefficients [40] [41].

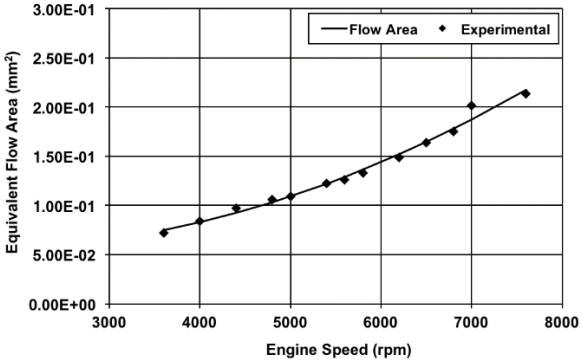

Figure 14: Equivalent flow area for injector nozzle vs. engine speed. The polynomial relationship for equivalent flow area and the experimental data are plotted

Apex Seal Leakage

Utilising the apex leakage facility within BOOST an initial sensitivity study was conducted on the baseline rotary model. Assuming that the effective leakage area was constant throughout the entire curve of the housing an initial sweep of 0 to 1 mm^2 with a resolution of 0.1 mm^2 was conducted which aligns broadly with the findings presented by Eberle [37].

Figure 15 shows the percentage change to wide open throttle (WOT) torque for differing engine speeds. It is apparent that apex seal leakage has significantly more impact at engine speeds below 6000rpm. A further sweep at 7000rpm from 0 to 0.1mm^2 suggested that an apex seal leakage area of 0.03mm^2 would result in improved rotary engine model fidelity.

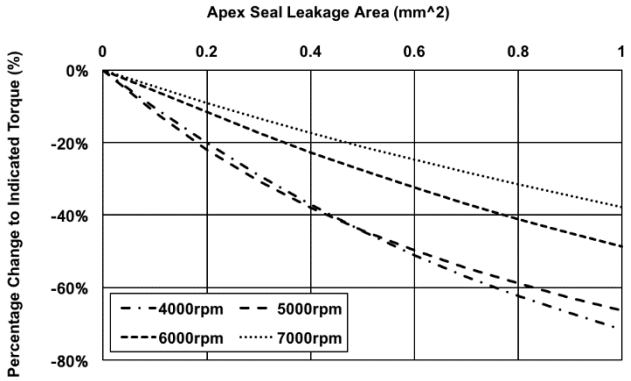

Figure 15: Percentage change to engine torque at WOT for different apex seal leakage areas and engine speeds

Results and Analysis

Model Validation

In order to validate the model, the power and torque output of each model (rotary and reciprocating) was calculated over a range of engine speeds and then compared with experimental data for the 225CS engine. The intake and exhaust connections used on the test stand and ambient conditions of the test chamber were input into the model. To establish effective pressure values, a simulation time of fifteen operational cycles was specified for each of the sixteen speed values recorded from 5000 rpm to 7500 rpm.

Figure 16 and Figure 17 show that both models fit the experimental data well, with the rotary model following the experimental data more closely. In Figure 18 the discrepancy (in percent) of the torque output from each model is compared to the experimental data, over the engine speed range tested. The average discrepancy of the reciprocating model was 7%, while the same values for the rotary model were much lower at 2.5%. The discrepancy for both models increases towards the two extremes of the simulated speed range.

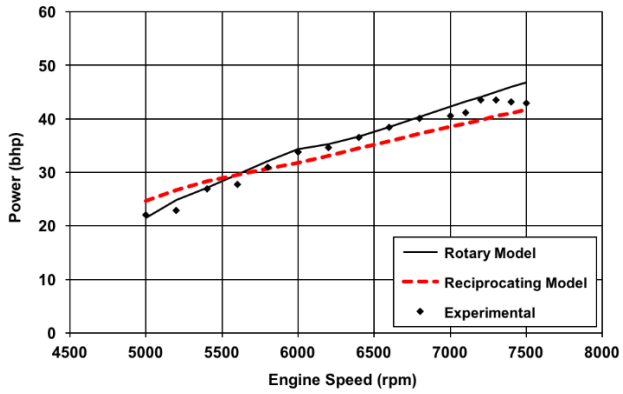

Figure 16: Power of the rotary and reciprocating model compared with experimental data vs. engine speed

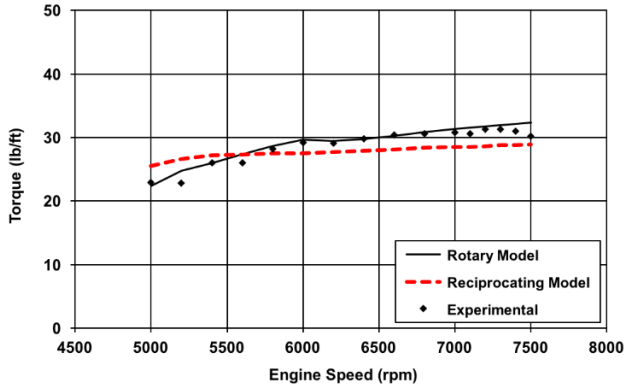

Figure 17: Torque of the rotary and reciprocating model compared to experimental data vs. engine speed

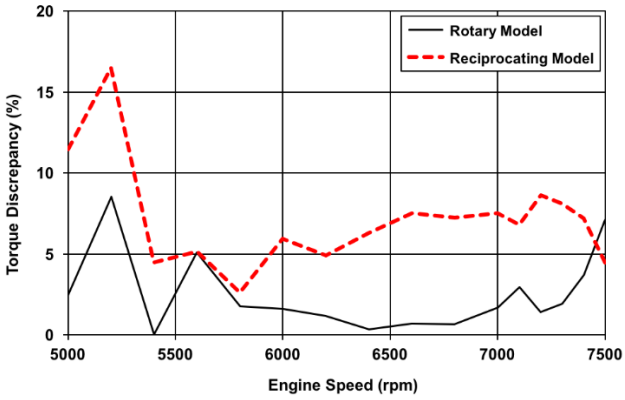

Figure 18: Percentage discrepancy in torque for rotary and reciprocating engine models compared to experimental data vs. engine speed

Limitations of Direct Injection

In this work, the angles used to define injector position refer to the location of the leading apex of a chamber after it passes top dead centre firing. Defining the minimum and maximum point on the epitrochoidal housing at which fuel could be injected was decided based on the following arguments. The minimum point on the housing at which the injector could be positioned was set at 237° since in theory fuel could be injected the moment the intake port opens, whereas the maximum point of injection will be at the last point before the injector would be present in the working chamber during combustion. This is because a low-pressure injector would likely not be able to withstand the high temperature and pressure conditions experienced in a combustion event. Therefore, since the start of ignition is at 18° before top dead centre, the latest point corresponded to 709° of eccentric shaft rotation after top dead centre firing.

As measured from the engine, the exhaust port closes at an eccentric shaft angle of 597° after top dead centre firing. Injecting fuel while the exhaust port is open would result in high unburned hydrocarbon (HC) emissions. Therefore, although it is possible to position the injector before 597° the model does not allow fuel to be injected until the exhaust port has been closed. Thus, placing the injector considerably before this angle will shorten the timing window for injecting fuel into the chamber. Consequently, a minimum position of 400° was selected for the simulation.

Although the maximum position for the injector was stated as 709°, by this point in the cycle the pressure inside the working chamber rises considerably due to compression making injecting fuel either difficult or impossible. Therefore, a maximum injection position of 700° was specified for the simulation.

Figure 19 shows the injector at position 597° with a line indicating the range of the injection points on the housing used in the simulation. It is worth noting that an injector placed between 464° and 510° would have to be placed off centre to account for the intake port.

A further explanation of injector position relative to eccentric shaft angle can be found in Appendix II.

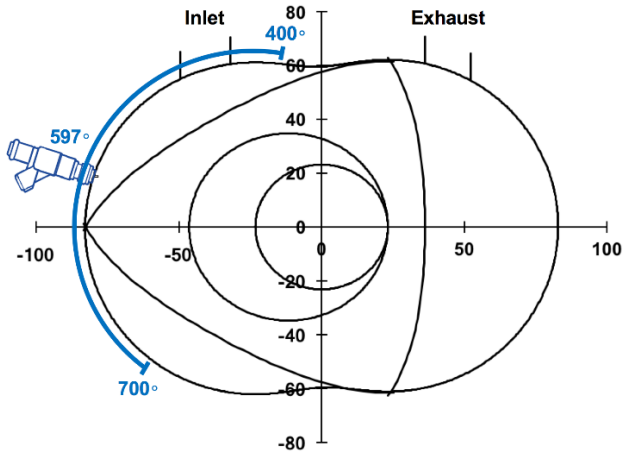

Figure 19: Cross-section of Wankel engine with representation of the range of injector positions simulated using data from the rotary model. Note that in this view the rotor is rotating counterclockwise

The mass flow of fuel per cycle for a range of injection positions and injection pressures at 5000 and 7500 rpm is shown in Figure 20 and Figure 21 respectively. The area of the surface plot marked in blue illustrates where the desired air/fuel ratio of 14.5 has been achieved and the grey area indicates where the mixture is lean due to insufficient injection. From both these graphs it is apparent that the current injection pressure (regulated at 3 bar) is insufficient to supply the required fuel into the chamber at both 5000 and 7500 rpm.

From Figure 20 and Figure 21 it is possible to see that the required injection pressure increases and the range of acceptable injector points narrows as the engine speed is increased from 5000 to 7500 rpm. It may also be observed that ~600° appears to be the injection point at which the greatest volume of fuel was able to be injected into the working chamber. Analysis of Figure 22 and Figure 23 reveals that an optimum injection point of 597° is true for any engine speed and any injection pressure.

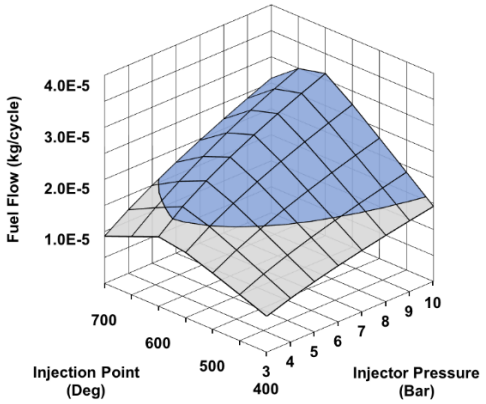

Figure 20: Fuel flow through injector nozzle per cycle vs. point of injection and injection pressure at 5000rpm. Darker-shaded area marked illustrates the conditions where the required air/fuel ratio was achieved

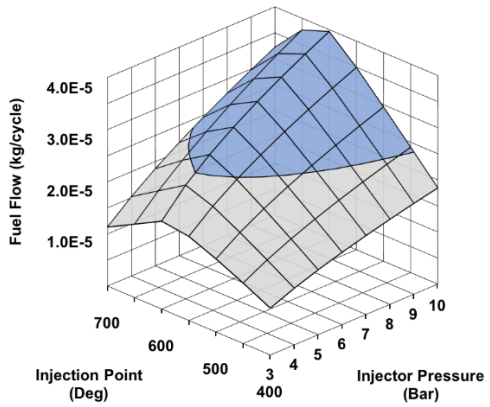

Figure 21: Fuel flow through injector nozzle per cycle vs. point of injection and injection pressure at 7500rpm. Darker-shaded area marked illustrates the conditions where the required air/fuel ratio was achieved

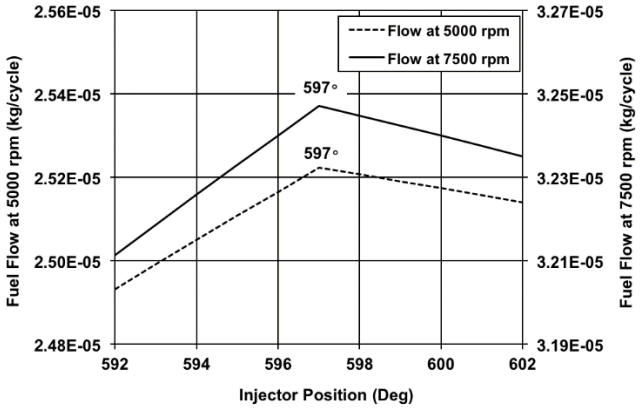

Figure 22: Fuel flow from the injector vs. injector position at 5000 and 7500rpm at 7 bar injection pressure

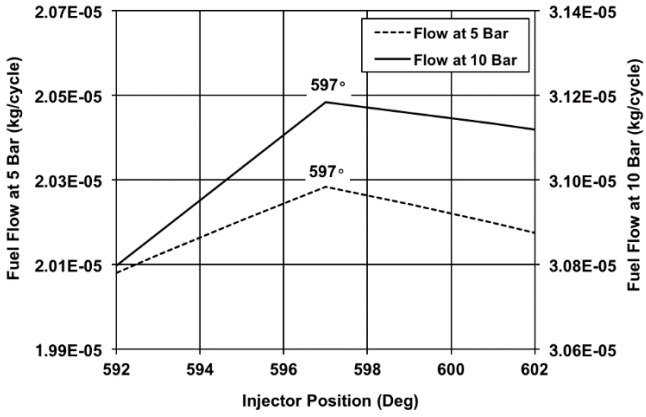

Figure 23: Fuel flow from the injector vs. injector position with injection pressures of 5 and 10 bar at a constant engine speed of 5000 rpm

Apex Seal Leakage

Taking apex seal leakage area into account the rotary model torque prediction more closely matched the experimental data, the effect of which across the engine speed range can be seen in Figure 24. Whilst the degradation in accuracy is still present at the extremes of engine speed, by taking apex seal leakage (of 0.03mm^2) into account, the co-efficient of variation of torque relative to experimental data dropped from 0.92 to 0.85. The effect on torque can be seen in Figure 25.

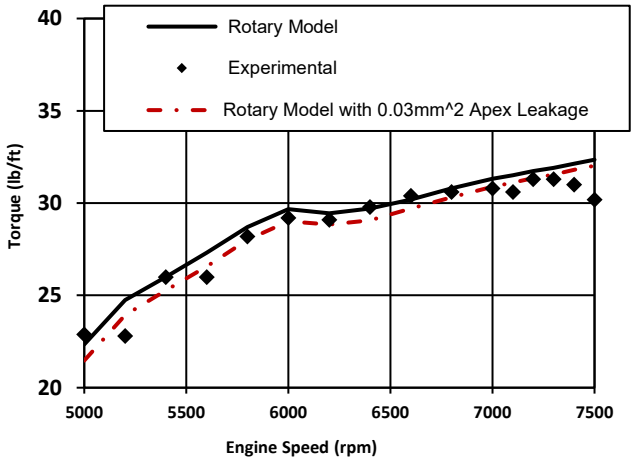

Figure 24: Comparison of experimental engine torque and rotary model prediction with and without 0.03mm^2 apex leak leakage area

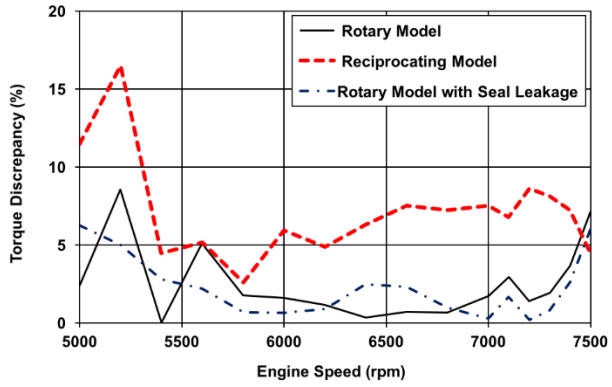

Figure 25: Percentage error of model torque predictions when compared to experimental data, for equivalent reciprocating engine, rotary engine, and rotary engine with representative seal leakage models

Discussion

Model Fidelity

Both the reciprocating and rotary models proved sufficient for modelling the performance of the 225CS Wankel engine. The model developed using the rotary domain of the software produced results that more closely fitted the experimental data, compared to the equivalent reciprocating engine model. However, the development of the models relied upon several assumptions due to the limited availability of data from engine tests, many of which were not available for the 225CS.

The significant influence of heat transfer on the engine performance was substantiated by the sensitivity analysis performed earlier. However, the accuracy of the heat transfer model used here was inhibited by a lack of experimental data. Therefore, further calibration of the heat transfer model using measured data is required to produce a more representative model. In addition, since the heat transfer depends directly on the surface area of the working chamber, a mathematically derived approach for defining the instantaneous epitrochoidal area (rather than the approximation method used here) is likely to improve the accuracy of the model.

Leakage is a significant source of power and efficiency loss in a Wankel engine due to the complex sealing system that is required compared with a conventional reciprocating engine. Here experimental data allowed the model to account for the peculiarities of the AIE SPARCS design. However, the assumption of a blow-by gap based on a reciprocating relationship was a major simplification and future work should consider obtaining empirical data from the engine via a leakdown test or equivalent.

Furthermore, a feature in BOOST that was not fully utilised in this work was one that considers the leakage between combustion chambers. The initial sensitivity study highlighted the well known susceptibility of Wankel engines to apex seal leakage, and while an assumption of a constant seal leakage area across the full curve of the housing path does improve the model accuracy for wide open throttle more work is required to fully establish the extent of the exchange of gases and loss of pressure between combustion chambers. To accurately define such leakage would require additional pressure tests and data regarding openings in the housing for spark plugs and potential injectors.

Finally, a motoring test would provide the model with a representative relationship for the frictional losses over the speed range of the engine, thus negating the requirement for an ambiguous prediction based on a 2-stroke engine, as was used here.

Heat transfer, leakage and friction are three main areas that ought to be the focus of future work to improve the accuracy of the model. However, despite the effects of the assumptions made here the discrepancy of the rotary model output in its current form is either equivalent or improves upon the results of previous efforts to model rotary engines using reciprocating engine software, such as those by Tartakovsky *et al.* [4] and Wendeker *et al.*[*21*].

Direct Injection

There are characteristics of the Wankel engine that potentially lend themselves well to DI, such as a longer injection window and high chamber turbulence for fuel-air mixing. In conventional DI reciprocating engines the window in which fuel can be injected is considerably shorter than for conventional PFI systems due to the nature of the valve timing and cycle duration. Since the fuel must be injected in such a short space of time (and to aid with mixing), injection pressures beyond 100 bar are often required even at low engine speeds and loads [42]. Here it was found that the slower cycle characteristic of the Wankel engine negates the requirement for such high pressures since the timing window is extended and the inherent high turbulence levels experienced in the working chamber of the Wankel engine should aid with mixing.

In addition, the physical shape of the Wankel engine make it especially suitable for applying DI. For example, in a typical reciprocating engine the options for positioning an injector are limited due to packaging constraints in the roof of the combustion chamber because it is necessary to also accommodate valves and a spark plug. On the other hand, the Wankel engine has an extensive range of potential injection points on the epitrochoidal housing, as highlighted in Figure 19. Furthermore, the unique characteristic of the moving combustion chambers allows a single injector to supply three working chambers, whereas in a conventional reciprocating DI engine individual injectors are required for each cylinder supplied via a pressurised common rail [38].

AIE are looking to apply low pressure DI to minimise the auxiliary load of the fuel pump. Although the current injector with its regulated pressure of 3 bar proved insufficient, pressures >4.5 bar could supply the desired fuel in the injection window at the maximum speed simulated (7500 rpm). This pressure is still well within the range of what is considered 'low pressure' and an order of magnitude less than current injection systems used on conventional reciprocating DI engines. However, if the current injection pressure is inflexible and must be retained at 3 bar, an alternative solution would be to introduce a second injector, which is relatively simple to do.

The optimum injection point on the epitrochoidal housing for delivering the most fuel was 597° of eccentric shaft rotation after top dead centre firing, irrespective of injection pressure or engine speed. This point corresponds directly with the point at which the exhaust port closes. Preventing fuel injection until after the exhaust port has closed in this way is desirable since mixture formation after scavenging has the potential to increase the absolute heating value of the trapped mixture resulting in higher BMEP, thus improving efficiency and increasing the power output [38].

The SPARCS integrated heat exchanger located within the rotor housing of the 225CS may make it impossible to locate an injector in the optimum position on the epitrochoidal housing, in which case an injector mounted on the side housing would have to be considered. This would require reducing the timing window for a given position as the model would have to consider the period of rotation where the injector would be covered by the face of the rotor, with this period increasing the further from the epitrochoidal housing the injector is placed. However, again, the use of two injectors would simply mitigate this problem.

As this work only focused on determining the limitations of direct injection regarding injection pressure and position, the actual benefits gained from applying DI were not analysed here. However, cooling of the combustion charge due to the evaporation of the fuel would likely increase power output and introducing the fuel into the air after scavenging has finished should improve that proportion of the peripherally-ported Wankel's currently poor fuel conversion efficiency that arises directly from fuel short-circuiting [43].

Conclusion

Two methods of modelling Wankel engines were used and although both were corroborated by experimental results the model created in the dedicated rotary engine modelling environment of AVL BOOST proved most reliable and was therefore used in a preliminary analysis of the application of direct injection to this engine concept. Further calibration is required to improve the fidelity of the model and ideally this should be guided by empirical data. This would help to reduce the number of assumptions made to create the model.

Direct injection has provided significant performance and fuel economy enhancements for conventional reciprocating engines and may offer a means by which to improve the Wankel engine.

Analysing the working chamber pressure trace from the model for different engine speeds proved that supplying the engine with low pressure direct injection is possible. With the EV-14 Bosch injector at the optimum position, injection pressures as low as 4.5 bar were capable of supplying the required fuel at all engine speeds. Thus, the current 3 bar pressure used for the PFI system would be inadequate to provide the required fuel, especially at high engine speeds. According to the approach used here the ideal injector position on the epitrochoidal housing for the AIE 225CS would be aligned with the leading edge of the rotor at 597° of eccentric shaft rotation after top dead centre firing.

The focus of future work should be firstly to improve the fidelity of the engine model (particularly in the areas of heat transfer, leakage and friction), and secondly to analyse the influence of the injection pressure, injection angle and combustion chamber shape on the mixing characteristics, using AVL FIRE or an equivalent CFD combustion analysis software package.

References

1. Dark, H.E., "The Wankel Engine: Introduction and Guide", 1st Ed. Ontario: Fitzhenry and Whiteside Ltd., 1974
2. Faith, N., "The Wankel Engine: The Story of the Revolutionary Rotary Engine", 1st Ed., London: George Allen and Unwin Ltd., 1976
3. Hege, J., "The Wankel Rotary Engine: A History", 1st Ed. Jefferson, North Carolina: McFarland and Company Inc., 2006
4. Tartakovsky, L., Baibikov, V., Gutman, M., Veinblat, M., et al. "Simulation of Wankel Engine Performance Using Commercial Software for Piston Engines," SAE Technical Paper 2012-32-0098, 2012, doi: 10.4271/2012-32-0098
5. Widener, S.K., Belvoir, F., "A Survey of Technology for Hybrid Vehicle Auxiliary Power Units," Interim Report TFLRF No. 311, Fort Belvoir, Virginia, 1995.
6. Yamamoto, K., "Rotary Engine," Hiroshima, Japan: Sankaido Co. Ltd., 1981.
7. Wladyslaw, M., "Modelling and Simulation of Working Processes in Wankel Engine with Direct Hydrogen Injection System," *Combustion Engines,* vol. 161, no. 2, pp. 42-52, 2015
8. Chis, A.R., "How Wankel's rotary engine works," Autoevolution, [Image Reference] Available: https://www.autoevolution.com/news/how-wankels-rotary-engine-works-19241.html. [Accessed: 29 August 2017]
9. Jones, C., "Clean Air: The Policies and Politics of Pollution Control," London: Feffer and Simons, 1975
10. DEFRA and Department for Transport (DfT), "UK Plan for tackling roadside nitrogen dioxide concentrations," July 2017
11. European Union, "Regulation (EU) No. 333/2014 of the European Parliament and of the council of 11 March 2014 amending regulation (EC) No. 443/2009 to define the modalities for reaching the 2020 target to reduce CO2 emissions from new passenger cars," *Official Journal of the European Union*, Vol. 57, pp. 15-21, 2014.
12. European Environment Agency (EEA), "Monitoring of CO2 emissions from the passenger cars – Regulation 443/2009," 20 April 2017 [Online]. Available:

https://www.eea.europa.eu/data-and-maps/data/co2-cars-emission-12. [Accessed 4 October 2017]
13. Butti, A., Delle Site, V., "Wankel Engine for Hybrid Powertrain," SAE Technical Paper 951769, SAE International, 1995, doi: 10.4271/951769
14. Noga, N., "Application of the internal combustion engine as a range-extender for electric vehicles," *Combustion Engines*, vol. 154, pp. 781-786, 2013.
15. Corolla, D., Ed. Automotive Engineering – Powertrain, Chassis, Systems and Vehicle Body, 1st Ed., Oxford: Elsevier Inc., 2009
16. Woodyard, D., "Exhaust Emissions and Control," in *Pounder's Marine Diesel Engines and Gas Turbines,* Burlington, Elsevier Science, pp. 61-86, 2009
17. Robert Bosch GmbH, Bosch Automotive Handbook, 9th Ed., Germany: Robert Bosch GmbH, 2014.
18. Frere, P., "Mercedes-Benz C111 Experimental Cars, Switzerland: Edita Lausanne, 1981.
19. Jones, C., Mount, R.E., "Design of a high-performance rotary stratified-charge research aircraft engine," 1984
20. Peden, M., "Study of Direct Injection Limitations on a Wankel Engine", M.Sc. Dissertation, University of Bath, UK, 30th August, 2017
21. Wendeker, M., Grabowski, L., Pietrykowski, K., Margryta, P., "Phenomenological model of a Wankel engine," PTNSS-2011-SC-014, 2011. English translation can be found in chapter 8 of the following: Szlachetka, M., Bialy, M., "The modelling of the external characteristics of the wankel engine," in *AVL Simulation Tools – Practical Applications*, Lublin, Lublin University of Technology, pp. 78-87, 2012.
22. Ansdale, R.F., "The Wankel RC Engine – Design & Performance," London: Iliffe Books Ltd., 1968.
23. Tomlinson, A., "Modelling of Wankel Engine Performance in Commercial Piston Engine Software," University of Bath, 2016
24. Heywood, J.B., Internal Combustion Engine Fundamentals, vol. 21, London: McGraw-Hill, 1988.
25. Suyabodha, A., Pennycott, A., Brace, C.J., "A preliminary approach to simulating cyclic variability in a port fuel injection spark ignition engine," *Proceedings of the Institute Mechanical Engineers, Part D: Journal of Automobile Engineering,* vol. 227, no. 5, pp. 665-674, 2012.
26. Norman, T.J., "A performance model of a spark ignition Wankel engine: including the effects of crevice volumes, gas leakage and heat transfer," Massachusetts Institute of Technology, Massachusetts, 1983.
27. Georgios, Z., "Mathematical and numerical modelling of flow and combustion processes in a spark ignition engine," Department of Applied Mathematics, University of Wisconsin, 2005
28. Armstead, J.R., Miers, S.A., "Review of waste heat recovery mechanisms for internal combustion engines," *Journal of Thermal Science and Engineering Applications,* vol. 6, no. 1, p. 014001, 2014.
29. Woschni, G., "A universally applicable equation for the instantaneous heat transfer coefficient in the internal combustion engine," SAE Technical Paper 670931, SAE International, 1967, doi: 10.4271/670931
30. Ramos, J.I., Internal Combustion Engine Modelling, CRC Press, 1989
31. Swanger, D.C., Walther, D.C., Pisano, A.P., "Small-scale rotary engine power system development status," Western States Section – Combustion Institute, University of California, Berkley, 2004
32. Nathan, S., "Innovation in the UK niche vehicles sector," 15 August 2014. [Online]. Available: https://www.theengineer.co.uk/issues/august-2014-online/innovation-in-the-uk-niche-vehicles-sector/ [Accessed August 2017].
33. MAHLE GmbH, Pistons and Engine Testing, 2nd Ed., London, New York: Springer Heidelberg Dordrecht, 2016
34. Popular Mechanics, Complete Car Care Manual, New York: Hearst Books, 2005.
35. Danieli, G.A., Keck, J.C., Heywood, J.B., "Experimental and Theoretical Analysis of Wankel Engine Performance," SAE Technical Paper 780416, 1978.
36. Blair, G., Design and simulation of two-stroke engines, Wallendale: SAE, 1996.
37. Eberle, M.K. and Klomp, E.D., "An Evaluation of the Potential Performance Gain from Leakage Reduction in Rotary Engines", SAE technical paper 730117, SAE 1973 World Congress Detroit, MI, USA, 1st February, 1973, doi: 10.4271/730117
38. Cornel, S., Direct injection systems for spark-ignition and compression-ignition engines, SAE International, 2000.
39. Bosch Engineering GmbH, "Injection Valve EV 14," 17 November 2016 [Online]. Available: http://www.bosch-motorsport.com/media/catalog_resources/Injection_Valve_EV_14_Datasheet_51_en_2775993867pdf.pdf. [Accessed 30 August 2017].
40. Mitroglou, N., Nouri, J.M., Gavaises, M., Arcoumanis, C., "Spray Characteristics of a multi-hole injector for direct-injection gasoline engines," *International Journal of Engine Research,* vol. 7, no. 3, pp. 255-270, 2006.
41. Rakshit, S., "High speed flow simulation in fuel injector nozzles," University of Massachusetts, Amherst, 2012.
42. Fiengo, G., di Gatea, A., Palladino, A., Giglio, V., Common rail system for GDI engines: modelling, identification and control, London: Springer, 2013.
43. Borretti, A., "Modelling unmanned aerial vehicle jet ignition Wankel engines with CFD/CFD," *Advances in Aircraft and Spacecraft Science,* vol. 2, no. 4, pp. 445-467, 2015.
44. Garside, D., "Rotary piston internal combustion engine", EP 2240671 B1, April 15, 2015.

Contact Information

Matthew Turner
Research Assistant
Dept Mechanical Engineering
University of Bath
Claverton Down
Bath
BA2 7AY
United Kingdom

m.turner@bath.ac.uk

Dr James Turner
Professor of Engines and Energy Systems
Dept Mechanical Engineering
University of Bath
Claverton Down
Bath
BA2 7AY
United Kingdom

j.turner@bath.ac.uk

Acknowledgments

Some of the work reported in this study has been funded by the Advanced Propulsion Centre UK as part of the ADAPT project, and the authors wish to gratefully acknowledge their financial support. As well as the University of Bath and AIE, project partners in ADAPT include Westfield Sportscars, Saietta, and General Engine Management Systems (GEMS). Thanks are also due to David Garside at CREL Ltd. whose patent Rotary Piston Internal Combustion Engine forms the basis of the AIE SPARCS cooling system [44].

Definitions/Abbreviations

Geometric Parameters

A	Working chamber surface area
a	Radius of apex seal
a'	Extension of rotor to accommodate apex seal
A_L	Rotor lobe area
A_S	Side housing area
A_E	Epitrochoidal housing area
B	Cylinder bore diameter
b	Rotor housing depth
e	Eccentricity
R	Generating radius
R_x	Equivalent rotor lobe radius
s	Cylinder area
S_p	Minimum clearance
V_c	Combustion chamber volume (reciprocating engine)
V_{recess}	Combustion chamber recess volume
V'	Working chamber volume
V'_{min}	Minimum working chamber volume
β	Rotor lobe half angle
λ	Connecting rod length
φ_{max}	Maximum angle of oscillation

Injection Parameters

A	Nozzle flow area
D_d	Discharge coefficient
P_{inject}	Injection pressure
$P_{chamber}$	Working chamber pressure
V	Volume flow rate of fuel
ρ	Fuel density

Model Parameters

a	Combustion completeness constant
BMEP	Brake mean effective pressure
DI	Direct Injection
FMEP	Friction mean effective pressure
IMEP	Indicated mean effective pressure
L_{st}	Stoke length (reciprocating engine)
N	Engine speed
x_b	Cumulative mass fraction
θ	Shaft angle
θ_0	Start of combustion
$\Delta\theta$	Combustion duration
η_m	Mechanical efficiency

Appendix I

Parallel trochoid curve (housing):

$$x = e\cos\alpha + R\cos\frac{\alpha}{3} + a\cos\left(\frac{\alpha}{3} + \varphi\right) \tag{13}$$

$$y = e\sin\alpha + R\sin\frac{\alpha}{3} + a\sin\left(\frac{\alpha}{3} + \varphi\right) \tag{14}$$

Parallel inner envelope (rotor):

$$X = R\cos 2\upsilon + \frac{3}{2}\cdot\frac{e^2}{R}(\cos 8\upsilon - \cos 4\upsilon) \pm e(\cos 5\upsilon + \cos\upsilon)\cdot\left(1 - \frac{9e^2}{R^2}\sin^2 3\upsilon\right)^{0.5} \pm \frac{3}{2}\ldots\cdot\frac{ea'}{R}(\cos 5\upsilon - \cos\upsilon) + a'\cos 2\upsilon\left(1 - \frac{9e^2}{R^2}\sin^2 3\upsilon\right)^{0.5} \tag{15}$$

$$Y = R\sin 2\upsilon + \frac{3}{2}\cdot\frac{e^2}{R}(\sin 8\upsilon + \sin 4\upsilon) \pm e(\sin 5\upsilon - \sin\upsilon)\cdot\left(1 - \frac{9e^2}{R^2}\sin^2 3\upsilon\right)^{0.5} \pm \frac{3}{2}\ldots\cdot\frac{ea'}{R}(\sin 5\upsilon + \sin\upsilon) + a'\sin 2\upsilon\left(1 - \frac{9e^2}{R^2}\sin^2 3\upsilon\right)^{0.5} \tag{16}$$

Equivalent radius:

$$R_x = R - e + \frac{3eR}{R - 4e} \tag{17}$$

Half angle:

$$\beta = \tan^{-1}\left\{\frac{\sqrt{3}R}{\left(\frac{6eR}{R - 4e} + R + 2e\right)}\right\} \tag{18}$$

Stroke Volume:

$$V'_H = \sqrt{3}e(2R_1 + R_2)b \tag{19}$$

The volume of the combustion chamber:

$$V_{min} = \pi r^2 h_2 \tag{20}$$

Where r is the radius and h_2 is the clearance height of the cylinder.

rearrange for h_2 gives:

$$h_2 = \frac{V_{min}}{\pi r^2}$$

(21)

Surface area of the combustion chamber:

$$A_{min} = 2\pi r^2 + 2r\pi h_2$$

(22)

Substituting the relationship for h_2 gives:

$$A_{min} = 2\pi r^2 + \frac{2V_{min}}{r}$$

(23)

In cubic form:

$$(2\pi)r^3 - (A_{min})r + (2V_{min}) = 0$$

(24)

The cubic was then solved numerically for r using the surface area and volume of the combustion chamber of the Wankel engine. Once r was solved, h_2 and h_1 (stroke length) could be found by rearranging the equation for the combustion chamber volume shown above. The crank radius is then simply the stroke length divided by two.

The equation used for the instantaneous volume of a reciprocating engine was as follows [1]:

$$\frac{dV}{d\alpha} = V_c + \lambda s\left\{(1 - \sin\alpha) + \frac{1}{4\lambda}(1 + \cos 2\alpha)\right\}$$

(25)

where V_c was the volume of the combustion chamber, λ was the length of connecting rod/radius of crank and s was the area of the cylinder.

The instantaneous area of a flat head reciprocating engine combustion chamber can be derived from basic geometry as the following [2]:

$$\frac{dA}{d\alpha} = \frac{\pi B^2}{2} + \frac{4\left(\frac{dV}{d\alpha}\right)}{B}$$

(26)

Appendix II

Locating the injector around the housing, relative to the eccentric shaft angle:

0 degrees of eccentric shaft rotation equates to a rotor position where a rotor face is aligned to top dead centre firing.

The ideal injector position of 597° after top dead centre firing, is equivalent to an eccentric shaft position of 483° before top dead centre firing.

With the eccentric shaft at 483° before top dead centre firing the ideal injector position on the housing is aligned directly with the leading apex seal edge of the rotor face used to define 0 degrees of top dead centre firing.

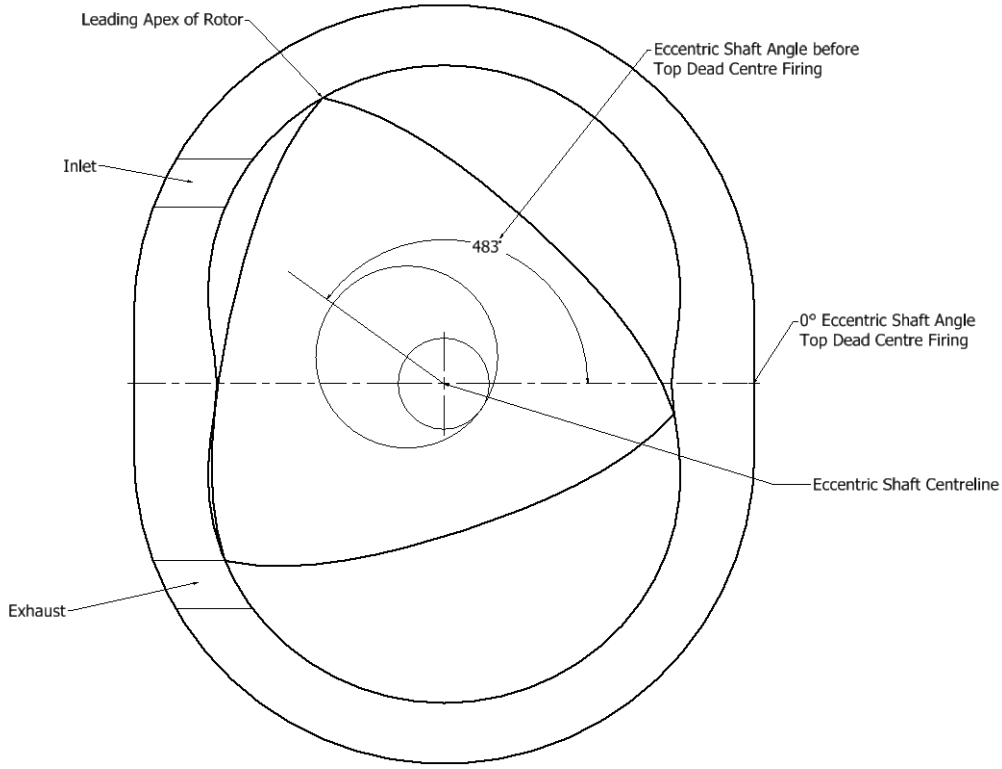

Figure 26 - Injector position relative to top dead centre firing. The injector is positioned in the housing in line with the leading apex rotor seal with the eccentric shaft positioned relative to top dead centre firing. 483° before top dead centre (TDC) firing is equivalent to 597° after TDC firing

Appendix III

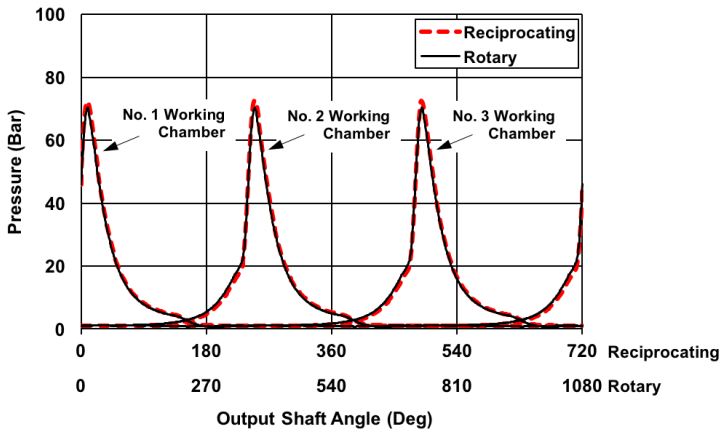

Figure 27: Pressure trace of all three working chambers for the rotary and reciprocating model at 5000 rpm with adjustment for different cycle lengths